

Exploring the Anti-Photoaging Potential of *Bacillus cereus* Superoxide Dismutase in New Zealand Rabbit Skin

Ana Indrayati^{1*}, Nurfitriyawatie¹, Rizal Maarif Rukmana^{2,3}

¹Faculty of Pharmacy, Universitas Setia Budi, Surakarta 57127, Indonesia

²Research Center for Pharmaceutical Ingredients and Traditional Medicine, National Research and Innovation Agency, Komplek Cibinong Science Center-BRIN, Cibinong, Bogor 16911, Indonesia

³Faculty of Health Science, Universitas Setia Budi, Surakarta 57127, Indonesia

ARTICLE INFO

Article history:

Received March 9, 2023

Received in revised form July 27, 2023

Accepted October 31, 2023

KEYWORDS:

Anti-photoaging,
Bacillus cereus,
liposomes,
rabbit's back skin,
SOD

ABSTRACT

Bacillus cereus is a heat-resistant bacteria that produces the enzyme superoxide dismutase (SOD). SOD is a metalloenzyme that can eliminate free radicals as the primary cause of photoaging. The point of this study is to find out how well *B. cereus* works as an anti-photoaging agent on the skin of rabbits' backs. The SOD enzyme was isolated from *B. cereus* using the colorimetric method and characterized for its activity. It was encapsulated by the liposome method, while the activity was measured on the rabbit's back skin exposed to ultraviolet-A (UV-A) radiation with the parameters of moisture, elasticity, and collagen levels using a skin analyzer. At the end of the treatment, a histological test for the animal skin was performed. The particle size analysis (PSA) results on the SOD in liposomes showed nanoparticles with an adsorption efficiency of 85.0% and a zeta potential of 28.0 ± 11.7 mV. SOD encapsulated in the liposomes also indicated anti-photoaging activity potential by increasing collagen, elasticity, and moisture levels. In addition, histological tests revealed that the collagen density in the SOD liposome treatment was higher than the negatively of control and normally of control but lower than the liposome collagen.

1. Introduction

Indonesia has over 17,000 islands, 86.7 thousand km² of coral reefs, and 88.5 million hectares of tropical forest and mangrove regions spanning 24,300 km² from Sabang to Merauke. Moreover, the country has the world's highest biodiversity after Brazil with a vast diversity of plant, animal, and microbiological species (Handayani *et al.* 2021). Microbes are abundant in numerous ecosystems, including acidic thermal springs, wetland forests, the Many Islands reef complex, Enggano Island, marine life, and traditional medicinal plant leaves (Liu *et al.* 2020). Meanwhile, bacteria are widespread organisms that can survive in freshwater, saline water, air, soil, and have symbiotic relationships with animals as well as plants (Liu *et al.* 2019). *Bacillus cereus* is an example of a bacteria with exceptional adaptability. This bacteria can adapt to hot settings, osmolarity fluctuations, nutrition and metabolite deprivation, together with oxidative

circumstances. It has evolved and survived numerous adaptations, including biofilm formation, swarming movement, as well as surfactin and metabolic enzyme production. Besides, the bacteria cells can adapt their physiology to changing external conditions to survive and reproduce (Duport *et al.* 2016). According to previous studies, *Bacillus cereus* is also capable of producing superoxide dismutase (SOD) (Zhang *et al.* 2020).

Bacteria can produce three types of SOD: the periplasmic Cu/Zn-SOD, the cytoplasmic Mn-SOD, and the Fe-SOD. Reactive oxygen species-induced oxidative stress can be mitigated by administering the SOD enzyme (Sun *et al.* 2021). The enzyme facilitates bacterial survival through the conversion of reactive oxygen species (ROS) that have been damaged into water and hydrogen peroxide (Najmuldeen *et al.* 2019). An imbalance between superoxide radicals and antioxidants can lead to elevated amounts of ROS in cells. Furthermore, oxidative stress might be induced by ROS, causing destroy of structures such as proteins, lipids, and nucleic acids. Inflammation,

* Corresponding Author

E-mail Address: anaindrayati@setiabudi.ac.id

fibrosis, genotoxicity, carcinogenesis (Dayem *et al.* 2017), atherosclerosis, hypertension, and other degenerative diseases are also connected with ROS (Bardaweel *et al.* 2018). High concentrations of ROS are one of the elements that might trigger the aging process in the skin (Treiber *et al.* 2012). Meanwhile, SOD is an antioxidant enzyme capable of maintaining homeostatic functions in the body. The enzyme can inhibit the expression of matrix metalloproteinases (MMPs), thereby inducing collagen synthesis and collagen production in the skin (Lee *et al.* 2021). This implies that SOD can also be utilized in anti-aging treatment (Younus 2018).

The skin plays a vital role in the human body as it is the primary barrier against pathogens (Richmond and Harris 2014). As a result of its anatomical positioning at the exterior boundary of the body, the skin is susceptible to various environmental factors, such as ultraviolet (UV) radiation emitted by the sun (Amaro-Ortiz *et al.* 2014). Furthermore, the primary factor contributing to the external aging of the skin, commonly referred to as photoaging, is prolonged exposure to ultraviolet (UV) light from the sun (Zhang and Duan 2018). The effects of UV radiation can be prevented by the presence of SOD (Kang *et al.* 2020). Previous studies have demonstrated that extracellular SOD can enhance collagen synthesis *in vitro* and *in vivo* as a preventive measure against skin aging (Lee *et al.* 2021). Moreover, recombinant superoxide dismutase (rSOD) from *Staphylococcus equorum* can enhance collagen deposition compared to cells without rSOD, which proves that rSOD has an anti-photoaging agent potential (Indrayati *et al.* 2016). The liposome is an ideal and safe drug delivery system with lipid bilayers mirror in the cell's plasma membrane (Filipczak *et al.* 2020). Encapsulation of medicine within liposomes boosts protection against bioactive chemicals, enhances medicinal efficacy as well as therapeutic index, and improves drug stability (Naibaho *et al.* 2019). Meanwhile, the skin's condition is a crucial indicator of age and health in daily living and photoaging has a significant impact on a person's quality of life (Porfire *et al.* 2009). Hence, the primary objective of this research is to examine the liposomal SOD activity of *B. cereus* as a potential anti-photoaging agent on the dorsal skin of rabbits based on collagen, elasticity, and moisture levels. It was motivated by the development of contemporary civilization and the increase in life expectancy.

2. Materials and Methods

2.1. Materials

The present empirical investigation was undertaken between January and June of 2021 using SOD enzymes obtained from . The bacteria were isolated from water in a mangrove forest in Maron Edupark, Semarang, Central Java. Additionally, the study employed six New Zealand rabbits with an average weight range of 2-4 kg and an approximate age of 7-8 months as experimental subjects. The assessment of anti-photoaging efficacy in animal models adheres to the guidelines set forth by the Health Research Committee of Dr. Moewardi, located in Surakarta, Indonesia (Decision letter: 213/II/HREC/2021). The hair of the animals was shaved on the back and divided into four parts. Nutrient Agar (N.A.), KCl, WST-1 solution, NaCl, KH₂PO₄, Bradford's reagent, Na₂HPO₄, Brain Heart Infusion (BHI), Coomassie Brilliant Blue, phosphate buffer, were obtained from Merck®; Darmstadt, Jerman. Meanwhile, Blood Agar Plate (BAP), Gram stain of *Bacillus cereus* Agar (BCA), Bovine Serum Albumin (BSA), and Water For Injection (WFI), were all acquired from Oxoid, Hampshire, UK. Sterile distilled water, phospholipids (Phospholipon 90G), ethanol P.A, cholesterol (Sigma), H₂O₂, Brain Heart Infusion Broth (BHIB), and rabbit blood plasma, were all purchased from Sigma/Aldrich, St. Louis, MO, USA.

2.2. Isolation of SOD Enzyme from *B. cereus*

Bacterial cells were broken down by mechanical method using sonication, followed by centrifugation. One to two Ose needles were taken from N.A. (Nutrient Agar) slant media before moving to 10 ml BHI media and incubating at 37°C for 24 hours to make a suspension of *B. cereus*. In addition, the enzyme extraction process involved the introduction of a 2% bacterial culture into a 300 ml BHI production media, followed by incubation at a temperature of 37°C for 24 hours (Priadi *et al.* 2018). The subsequent step consisted of harvesting the bacterial cells by centrifuging the growth medium at 5,000 rpm for 15 minutes and at 40°C to separate the cells from the supernatant, then the process was repeated three times. The pellet was resuspended in PBS solution, while the cells were disrupted using sonication. Sonication was performed at an amplitude of 50 for 5 minutes, with an interval of 1 minute at a temperature of 40°C. The suspension underwent a second round of centrifugation at a speed of 5,000

rpm for a duration of 15 minutes at a temperature of 40°C. The supernatant, produced after centrifugation, containing the crude extract of the SOD enzyme was transferred into a microtube and subsequently stored at a temperature of 40°C in a refrigerator (Dos Santos *et al.* 2000).

2.3. Determination of Total Protein Crude Extract of SOD Enzyme of *B. cereus*

The quantification of the overall protein concentration in the crude extract was conducted using the Bradford technique. This was performed by adding 4 µl of sample to 200 µl of Bradford reagent and adjusting up to 1 ml with distilled water. The absorbance measurement was conducted using a UV-Vis spectrophotometer at 595 nm (Stelder *et al.* 2018).

2.4. SOD Activity Analysis of *Bacillus cereus*

The activity of the superoxide dismutase enzyme isolated from *B. cereus* was measured by considering the value of the inhibition rate using the superoxide dismutase activity assay kit (colorimetry). The WST-1 from Merck® Darmstadt, Jerman was used, which produces a water-soluble formazan dye when reducing the superoxide anion. The superoxide dismutase activity test was divided into four parts: Sample (sample, Enzyme, and WST), Blank 1 (Enzyme, WST and H₂O), Blank 2 (buffer, sample, and WST), and Blank 3 (WST, sample, and buffer) (H₂O, WST, buffer). The components of the test and control solutions were listed in Table 1.

Superoxide dismutase extract of *Bacillus cereus* was prepared up to 20 µl, which was made in 3 replications. The sample solution and blanks 1, 2, and 3 were prepared with the composition according to Table 1. The solution was pipetted and put into plate well 96, then homogenized by gently shaking the microplate. The measurement of absorbance was conducted with a microplate reader set at 450 nm (Ukeda *et al.* 1999). The activity of Superoxide Dismutase (SOD) was quantified by determining the

inhibition rate as a percentage using the following formula (Novarini *et al.* 2020):

$$\% \text{ SOD activity} = \frac{(\text{blank 1} - \text{blank 3}) - (\text{Sample} - \text{blank 2})}{(\text{blank 1} - \text{blank 3})} \times 100\%$$

2.5. Liposome Encapsulation of *B. cereus* SOD Extract

Liposomes were prepared by homogeneously combining 50 M/ml of phosphatidylcholine and 25 M/ml of cholesterol with 5 ml of ethanol in a 300 ml round-bottom flask. The solvent underwent evaporation using a rotary evaporator under a pressure of 500 C, resulting in the formation of a thin lipid coating on the flask's surface. The thin film hydration technique was performed by utilizing 5 ml of *B. cereus* SOD enzyme extract with a concentration of 0.5 mg/ml in a phosphate buffer solution (PBS) with a pH of 7.8. The process was conducted using a rotary evaporator at a temperature of 37°C for a duration of 15 minutes. The liposomal dispersion formed was maintained at 40°C for one hour. Subsequently, the liposomes produced were sized uniformly using a sonicator for 8 minutes (Karn *et al.* 2013).

2.6. Liposome Characterization of SOD Extract from *B. cereus*

2.6.1. Size of Liposome Particles

An instrument (Horiba Scientific, Nano Particle instrument SZ-100) was used to measure the particle size. Particle size analyzer was read with preparations that had been top-down in size with a sonicator on PBS (Duraivel *et al.* 2014).

2.6.2. Determination of Zeta Potential

Liposome zeta potential was evaluated using a zeta-sizer on a Nano Particle Analyzer SZ-100. The samples were diluted by adding one drop to ten milliliters of the dispersion solution, namely a phosphate buffer with a pH of 7.4. Prior to measurements, the liposomes underwent two rounds of dilution with phosphate-buffered saline. Subsequently, the samples were transferred into a cuvette and subjected to analysis at a temperature of 25°C (Fan *et al.* 2021).

2.6.3. Quantifying the Effectiveness of Entrapment

The efficiency of entrapment was determined by centrifuging a mixture of 5 milliliters of SOD enzyme

Table 1. Composition of sample and blank solutions

	Sample (µl)	Blank 1(µl)	Blank 2(µl)	Blank 3(µl)
Sample	20	-	20	-
WST reagent	200	200	200	200
Buffer	-	-	20	20
ddH ₂ O	-	20	-	20
Enzyme reagent	20	20	-	-

liposome and 5 milliliters of 0.05 M potassium phosphate buffer at 3,500 rpm for 30 minutes. The 1 ml supernatant was taken and diluted in a measuring flask using distilled water to 25 ml. In addition, a volume of 1.0 ml from the solution above was further diluted by adding distilled water to get a final volume of 25 ml. The measurement of solution absorption was conducted utilizing a UV-Vis spectrophotometer at the wavelength corresponding to the maximum absorption. Subsequently, the concentration of the solution was determined by employing the equation derived from the calibration curve. This enabled the determination of the concentration of the free drug (FD). The calculation of entrapment efficiency was performed utilizing the prescribed formula:

$$\% EE = \frac{TC - FD}{TC} \times 100\%$$

Definition:

TC = The formula contains the total amount of chemical

FC = The quantity of chemicals identified in the supernatant (excluding entrapment) (Lujan *et al.* 2019)

2.7. The Anti-photoaging Activity of SOD Liposome Extracted from *Bacillus cereus* on the New Zealand Rabbits

2.7.1. Acclimatization of Experimental Animals

A total of six male New Zealand rabbits, with weights ranging from 2 to 4 kg and ages between 7 and 8 months, were procured from the Pharmacology Laboratory at Setia Budi University in Surakarta, Indonesia. The test animals were provided with a cage and acclimated for one week. The cage was placed under the standard laboratory conditions of 25±2°C ambient temperature, a 12-hour cycle of light and darkness and 55±5 percent relative humidity (Lee *et al.* 2014). They were fed pellets on a regular basis and had full access to water. The animal testing procedures adhered to the guidelines set forth by the Health Research Committee of Dr. Moewardi General Hospital, Indonesia, and conformed to established norms.

2.7.2. Induction of Skin Aging by UV-A Irradiation

The posterior fur of the rabbit has been trimmed and segmented into four equal sections, each

measuring 2 cm in diameter (Manosroi *et al.* 2012). The rear skin of the rabbit was exposed to Exoterra® Daylight Basking Spot, a source of ultraviolet (UV) radiation. The light source was illuminated for two weeks, with a cumulative dose of 64.69 J.cm⁻² per hour (Chen *et al.* 2019). The skin is analyzed to determine the proportion of collagen, elasticity, and moisture.

2.7.3. Application of *B. cereus* SOD Liposomes to Rabbits Following UV-A Radiation

Liposomes containing and without SOD and collagen were applied to the rabbit's back daily for the next 28 days (Suksaeree *et al.* 2018). The analysis of the rabbit skin was conducted after the end of the treatment process. The rabbit's skin is captured in a photograph and transmitted to a computer for analysis using a skin analyzer (Lee *et al.* 2014).

2.8. Histology Examination of Rabbit Skin Following Treatment with SOD

Histological preparations were prepared from skin tissue collected after treatment completion, ensuring that the experimental animals were not harmed. The rabbit was taken from its cage and placed in a container containing a deadly dose of ether. The skin tissue utilized for each treatment was sectioned into dimensions of 2 × 2 cm, with a uniform thickness of half a centimeter. The tissue was later treatment with a 10% formalin solution, with the volume of formalin being ten times greater than the amount of tissue removed. The obtained skin sample was immersed in a solution containing 10% formalin and a neutral buffer for 24 hours. Furthermore, slices of biopsied or surgically removed tissue were formalin-fixed for 8 to 48 hours and deparaffinized with xylene. The sample was stained with Van Gieson dye for 1 minute and subsequently, the specimen was encased within paraffin, diced to a thick of one to twenty microns, re-stained, and examined under a olympus cx 23 microscope with a 40x objective lens magnification and a 10x eyepiece. Observations were conducted to determine the collagen fibers generated in the skin tissue (Chen *et al.* 2019).

2.9. Data Analysis

The statistical analysis of the research data was conducted using SPSS 17 software. The statistical methods employed in this study included the paired T-test and one-way ANOVA.

3. Results

3.1. Extraction of SOD Enzymes from *B. cereus*

The process of extraction of the superoxide dismutase (SOD) enzyme from *B. cereus* bacteria involved a series of sequential steps, including the bacteria's initial cultivation, subsequent harvesting of the bacterial cells, and the subsequent disruption of the cellular structure through sonication. The SOD enzyme is an intracellular enzyme that can be released from cells through the process of sonication, which causes cell lysis and subsequent extracellular release of the enzyme. The extraction of superoxide dismutase (SOD) enzyme from *B. cereus* bacteria yielded 11.3 ml, resulting in a volumetric yield of 3.7% v/v.

3.2. Determination of Total Protein

The quantification of the protein concentration in the *B. cereus* SOD enzyme extract was conducted by measuring the absorbance and applying a linear formula derived from the BSA curve standard. The standard curve yielded the equation $y = 0.0292x + 0.1075$ as the foundation for calculating the sample's protein. The total protein content of the SOD enzyme obtained from *Bacillus cereus* was 1.20 mg/ml.

3.3. SOD Enzyme Activity of *B. cereus*

The evaluation of SOD activity was judged by measuring the inhibition rate of SOD by utilizing the Superoxide Dismutase Activity Assay Kit, employing a colorimetric method. The SOD enzyme activity test results were expressed in percentage inhibition of anion superoxide and the results are $79.05\% \pm 2.62\%$.

3.4. Liposome Characteristics of SOD Enzyme from *B. cereus*

A sonication-modified thin-film hydration approach was used to produce liposomes from the SOD extract. The liposomes that were acquired were later analyzed for their size of particle, zeta potential, and absorption effectiveness. The findings of the size of the particle test, the potential zeta value, and the effectiveness of encapsulation are presented in Table 2.

3.5. The Results of UV-A Exposure on the Skin of the Rabbit's Back

The experiment involved subjecting rabbit test animals to two weeks of UV-A irradiation to evaluate their response to anti-photoaging measures. The application of UV-A irradiation led to a reduction in the levels of elasticity, moisture, and collagen, as indicated in Table 3.

3.6. Anti-photoaging Activity of SOD Liposomes of *B. cereus*

In anti-aging studies, increasing the levels of collagen, elasticity, and moisture are crucial elements. The increase after the treatment indicates that SOD liposomes have antiphotaging potential. The quantification of the rise in collagen content in rabbit skin after the administration of SOD liposomes can be ascertained by evaluating the area under the curve (AUC) grade. The findings presented in Table 4 demonstrate an increase in the relative concentration of collagen inside the dorsal skin of rabbits after the administration of SOD liposomes derived from *B. cereus*.

Treatment using SOD liposomes from *B. cereus* can increase the percentage of skin elasticity on the back of rabbits exposed to UV-A. An increase in the percentage of skin elasticity was indicated by higher AUC values as shown in Table 5.

The application of SOD liposomes on the dorsal skin of rabbits following exposure to UV A radiation resulted in a notable increase of over 10% in skin moisture levels, as seen by the data presented in Table 6.

3.7. Histological Results on Rabbit Dorsal Skin Tissue after Treatment with *B. cereus* SOD Liposomes

Histological observations were carried out using the van Gieson method to prove the increase in collagen density. The findings are illustrated in Figure 1 and presented in Table 7. The analysis was carried out using an opitlab tool, and the percentage of collagen density was calculated using the image J application. The

Table 2. Shows the size of the particle, potential zeta value and effectiveness of encapsulation of SOD liposomes from *B. cereus*

Liposome	Size of the particle (nm)	Potential zeta value (mV)	Effectiveness of encapsulation (%)
<i>Bacillus cereus</i>	148.16±21	28.0±11.7	85.0
Collagen (positive control)	126.7±4.2	50.17±4.4	-

Table 3. Prior to and following UVA radiation, lower levels of moisture, elasticity, and collagen

Kind of examining	Prior to UV-A irradiated	following UV-A irradiated	Reduction (%)
Moisture	11.61±1.52	7.62±1.14	34.48
Elasticity	61.82±1.92	55.63±1.34	10.03
Collagen	60.01±1.58	55.61±3.29	7.33

Table 4. Grade of Area Under the Curve (AUC) and collagen % increase

Type of treatment	Area under the curve grade	Increased collagen (%)
Normally of control	1707.23±22.71 ^{abd}	9.94
Negatively of control	1552.91±14.22 ^{bcd}	0.00
Liposome of <i>B. cereus</i>	1610.32±23.52 ^{abc}	3.70
Liposome of collagen	1777.04±41.82 ^{acd}	14.43

a: noticeably distinct from negatively of control, b: noticeably distinct from collagen liposome, c: noticeably distinct from normally of control, d: noticeably distinct from *B. cereus* liposome

Table 5. Area under curve data of elasticity and percentage increase of Elasticity

Type of treatment	Area under curve data of elasticity	Percentage increase of elasticity (%)
Normally of control	1703.52±22.32 ^{ad}	6.59
Negatively of control	1598.22±15.41 ^{bcd}	0.00
Liposome of collagen	1729.11±26.61 ^{acd}	8.19
Liposome SOD of <i>B. cereus</i>	1631.72±17.52 ^{abc}	2.10

a: drastically different from negatively of control, b: drastically different from collagen-containing liposome, c: drastically different from normally of control, and d: drastically different from liposome SOD of *B. cereus*

results on the liposome with UV-A treatment group showed collagen with the lowest density, followed by the liposome non UV-A treatment, liposome SOD enzyme of *B. cereus*, and the liposome of collagen.

Table 6. Area Under Curve Data and percentage increase of skin moisture

Group of treatment	Area under curve data of elasticity	Percentage increase of skin moisture (%)
Normally of control	347.04±18.51 ^{ad}	50.29
Negatively of control	230.91±15.42 ^{bcd}	0.00
Liposome of collagen	335.82±28.73 ^{ad}	45.45
Liposome SOD of <i>B. cereus</i>	254.03±22.82 ^{abc}	10.02

a: noticeably distinct from negatively of control, b: noticeably distinct from liposome of collagen, c: noticeably distinct from normally of control, d: noticeably distinct from liposome SOD of *B. cereus*

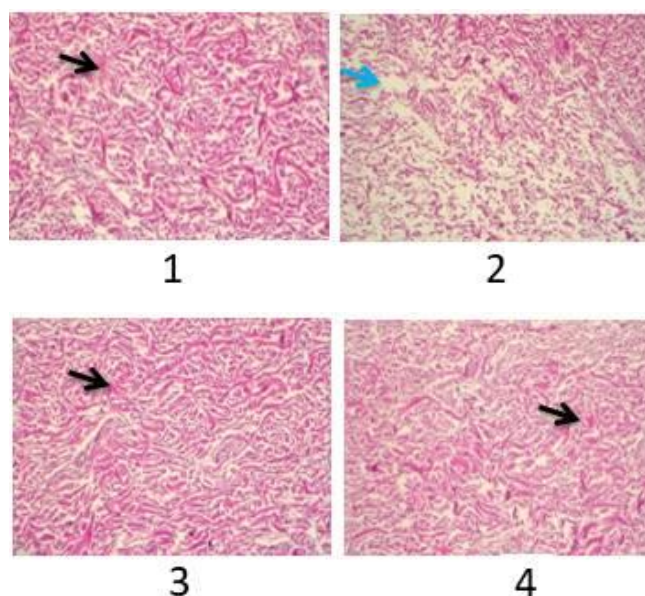


Figure 1. The histological image of rabbit skin connective tissue. 1: normally of control treatment type, 2: negatively of control treatment type, 3: liposome of collagen type, 4: liposome SOD *B. cereus* group, →: demonstrated collagen mass, →: demonstrated collagen being loosened

Table 7. Percentage of collagen density using imageJ.app

Type of treatment	Percentage of collagen density using imageJ.app (%)
Normally of control	23.71±1.65 ^{abd}
Negatively of control	17.84±1.77 ^{bcd}
Liposome of collagen	39.37±1.82 ^{acd}
Liposome SOD enzyme of <i>B. cereus</i>	31.10±0.42 ^{abc}

a: drastically different from negatively of control, b: drastically different from liposome collagen, c: drastically different from normally of control, d: drastically different from liposome SOD enzyme of *B. cereus* group

4. Discussion

Bacillus cereus is a bacterium known for its remarkable adaptability, as it can be found in diverse ecological niches such as soil, water, and both plant and animal environments. This bacterium is capable of thriving under different environmental stress conditions. This research demonstrated that the bacteria generates the enzyme superoxide dismutase, as proven by the extraction results, which yielded 11.3 ml (3.7% v/v) of the SOD enzyme. *B. cereus* can produce SOD because previous research identified genes encoding the formation of iron SOD (FeSOD) and manganese SOD (MnSOD). In *B. cereus*, the expression of the *sodC* and *sodB* genes can stimulate the formation of SOD (Wang *et al.* 2011). SOD was isolated from *B. cereus* bacteria, which thrive in an ideal environment at 37°C and pH 7, culminating in the highest extraction. Moreover, sonication induces alterations in the cellular membrane structure, resulting in the liberation of molecules and the diminishment of their sizes (Petkar *et al.* 2013). The SOD principal objective in cells is to guard against and minimize oxidative damage induced by reactive oxygen radicals. The activity test using the WST-1 method revealed that superoxide anion inhibition reached 79.05%±2.62%. This was similar to the activity of four forms of SOD including copper-zinc (CuZnSOD), iron (FeSOD), and manganese (MnSODA1 and MnSODA2) from *Klebsiella pneumoniae* bacteria against anion inhibition, which ranged from 51.67-82.82% (Najmuldeen *et al.* 2019).

The findings indicate that *B. cereus* exhibits robust superoxide dismutase (SOD) activity, surpassing a threshold of 50%. Superoxide dismutase (SOD) is an enzymatic antioxidant that facilitates the conversion of superoxide anion into hydrogen peroxide (H₂O₂) and oxygen (O₂), hence mitigating reactive oxygen species (ROS) activity (Najmuldeen *et al.* 2019). Radicalism caused by these free radicals can be reduced by the antioxidant SOD, which donates electrons to the free radicals, causing them to become stable. Furthermore, SOD potentially may function via impeding receptor activation, as well as suppressing the expression of AP-1 and MMP genes. It also stimulates collagen production by increasing TGF- β and procollagen gene expression (Indrayati *et al.* 2016). According to a recent study, the SOD enzyme from *B. cereus* exists in four forms namely copper-zinc, iron, and manganese (two forms) (Zhang *et al.* 2020).

In this study, the SOD enzyme derived from *B. cereus* was converted into nanopolymers by encapsulating it in liposomes as an antiaging medication (Azadmanesh and Borgstahl 2018). Liposomes have several advantages as drug delivery agents, including biodegradability, biocompatibility, non-toxicity, non-allergenicity, and non-irritability. Other advantages include nanoparticle size for easy absorption by cells, stable active ingredient content, high active ingredient content, and controlled release of the active substance (Vorauer-Uhl *et al.* 2001). SOD liposomes from *B. cereus* had the following characteristics: particle size of 148.16±21.00 nm, zeta potential value of 28.0±11.7, and encapsulation efficiency of 85.0%. The size of the SOD liposome particles, which are nanoparticles, caused an easy penetration into the cell. The smaller the particle size, the easier it will be to enter cells and boost body absorption (Shazeeb *et al.* 2014). According to recent studies, only particles with a size between 50 to 500 nm can permeate the skin, and smaller particles can easily breach the stratum corneum barrier (Hou *et al.* 2022). Furthermore, the zeta potential value was larger than 25 mV, indicating that SOD liposomes are highly stable. When the potential zeta value is high, colloids are less likely to flocculate and aggregate from tiny to massive sizes inside the cell. Particles can attract one another and form flocs when their potential zeta value is low. When the potential zeta value is low, the layer between particles is skinny, and the particles strongly tend to clump together (Honary and Zahir 2013). A colloid with a high potential zeta exhibits enhanced stability. Furthermore, the concept of potential zeta is utilized to assess the stability of a dispersion system, considering the prevailing repulsive or attractive forces. It is used to evaluate physical stability, surface coating effectiveness, or drug adsorption on nanoparticles (Yun *et al.* 2013).

Based on the results, the effectiveness of encapsulation of *B. cereus* SOD liposomes was 85%. It was measured to determine the polymer's ability to adsorb active compounds, the effectiveness of the procedure used, and to provide an idea of how much medicine was successfully absorbed into the nanoparticle system. Based on a prior investigation, the thin film dispersion technique synthesized elastic liposomes containing percutaneous melatonin transport (MLT), and further optimization was conducted utilizing the central composite design (CCD) methodology. As a result, the encapsulation

efficiency was found to be 73.91%. Considering that more than 70% of the chemical was absorbed in the nanoparticle system, the encapsulation efficiency findings can be considered good (Hou *et al.* 2022).

According to the findings, a two-week exposure of the rear skin of New Zealand rabbits to UV-A radiation leads to a reduction in moisture, collagen, and elasticity levels by around 34.48%, 7.33%, and 10.03%, respectively. UV exposure not only accelerates aging, but it can also cause skin lesions, diminish skin suppleness, and increase skin dryness, according to previous investigations. Chronic exposure to UV light can harm the elastic fibers of rat skin as well as the physiological structure of the tissue (Hou *et al.* 2022). A previous study found that UV-A can harden and reduce the suppleness of collagen gel. Collagen is produced by fibroblasts, hence, hardness and decreased elasticity indicate a decline in fibroblast collagen production. Furthermore, continuous UV-A exposure causes decreased collagen synthesis (Maeda 2018). Radiation exposure also induces the production of reactive oxygen species (ROS), which can stimulate cytokine receptors and growth factors located on the cell membrane of fibroblasts. The activation of receptors leads to the initiation of intracellular MAP kinase signaling pathways, ultimately resulting in the activation of the nuclear activation protein-one (AP-1) gene transcription factor complex. The overactivation of AP-1 in fibroblast cells leads to an upregulation of the MMP-1 (collagenase), MMP-3 (stromelysin), and MMP-9 (gelatinase) genes. These genes are responsible for collagen degradation and other proteins within the dermis. Furthermore, it has been demonstrated that the activation of AP-1 leads to a decrease in the expression of procollagen genes, resulting in a reduction in collagen formation (Budden *et al.* 2021)

The application of SOD liposomes to the rabbits' backs enhanced the percentage of collagen, elasticity, and skin moisture by 3.70%, 2.10%, and 10.02% respectively. The increase after the treatment delivery was significantly different from the negative control trial. The percentage of collagen density increased in histological observations with a value of 31.10 ± 0.42 which is greater than that of the negative and normal controls. This implies that SOD encapsulated in liposomes enhances the penetration of active compounds into epidermal layers, thereby increasing the percentage of collagen, elasticity, and hydration. Considering that liposomes have nanoscale sizes, active compounds are more easily absorbed through the skin

(Tran *et al.* 2022). A previous study demonstrated that liposomes can improve therapy outcomes by increasing the stability of active compounds (Bi *et al.* 2019). Previous research indicated that SOD liposomes from *Bacillus altitudinis* function as an anti-photoaging agent by increasing elasticity, moisture, and collagen content by 5.10%, 26.90%, and 6.46%, respectively. The histological analysis revealed that the application of SOD *B. altitudinis* liposomes resulted in a significant rise in collagen levels, reaching a value of 36.62% (Nurfitriyawatie *et al.* 2023a). The results of this investigation suggest that SOD liposomes obtained from *B. altitudinis* had enhanced efficacy in comparison to liposomes derived from *B. cereus*. This can be attributed to the higher content of SOD enzyme produced by *B. altitudinis*, which measured at 13.3 ml. The increased superoxide dismutase (SOD) content led to a higher SOD activity, specifically measuring at $85.09\% \pm 1.24\%$. Furthermore, the SOD liposomes derived from *B. altitudinis* exhibit specific attributes, such as a particle size measuring 112.96 ± 17.3 nm. Notably, this particle size is smaller than that of the SOD liposomes obtained from *B. cereus*. Reduced particle sizes facilitate the cellular uptake of active substances and enhance their absorption within the rabbits back skin (Nurfitriyawatie *et al.* 2023b).

In conclusion, the utilization of liposomes containing SOD *B. cereus* extract exhibits promising potential as an anti-photoaging agent when applied to the dorsal skin of rabbits. This is demonstrated by the observed effects of SOD *B. cereus* liposomes, which have been found to enhance collagen percentage, improve elasticity percentage, and increase skin moisture levels.

Acknowledgements

The author expresses gratitude to the Postgraduate Research Grant Program, Directorate General of Research, Ministry of Education and Culture of the Republic of Indonesia. The author expresses gratitude towards the pharmacology laboratory, microbiology laboratory, Setia Budi University in Surakarta, and the integrated laboratory at Yogyakarta State University.

References

- Amaro-Ortiz, A., Yan, B., D'Orazio, J.A., 2014. Ultraviolet radiation, aging and the skin: Prevention of damage by topical cAMP manipulation. *Molecules*. 19, 6202–6219. <https://doi.org/10.3390/molecules19056202>

- Azadmanesh, J., Borgstahl, G.E.O., 2018. A review of the catalytic mechanism of human manganese superoxide dismutase. *Antioxidants*. 7, 1-16. <https://doi.org/10.3390/antiox7020025>
- Bardaweel, S.K., Gul, M., Alzweiri, M., Ishaqat, A., Alsalamat, H.A., Bashatwah, R.M., 2018. Reactive oxygen species: the dual role in physiological and pathological conditions of the human body. *Eurasian Journal of Medicine*. 50, 193–201. <https://doi.org/10.5152/eurasianjmed.2018.17397>
- Bi, Y., Xia, H., Li, L., Lee, R. J., Xie, J., Liu, Z., Qiu, Z., Teng, L., 2019. Liposomal vitamin D3 as an anti-aging agent for the skin. *Pharmaceutics*. 11, 1-12. <https://doi.org/10.3390/pharmaceutics11070311>
- Budden, T., Gaudy-Marqueste, C., Porter, A., Kay, E., Gurung, S., Earnshaw, C. H., Roeck, K., Craig, S., Traves, V., Krutmann, J., Muller, P., Motta, L., Zanivan, S., Malliri, A., Furney, S.J., Nagore, E., Virós, A., 2021. Ultraviolet light-induced collagen degradation inhibits melanoma invasion. *Nature Communications*. 12, 1-13. <https://doi.org/10.1038/s41467-021-22953-z>
- Chen, X., Peng, L.H., Chee, S.S., Shan, Y.H., Liang, W.Q., Gao, J.Q., 2019. Nanoscaled pearl powder accelerates wound repair and regeneration *in vitro* and *in vivo*. *Drug Development and Industrial Pharmacy*. 45, 1009–1016. <https://doi.org/10.1080/03639045.2019.1593436>
- Dayem, A.A., Hossain, M.K., Lee, S. Bin, Kim, K., Saha, S.K., Yang, G.M., Choi, H.Y., Cho, S.G., 2017. The role of reactive oxygen species (ROS) in the biological activities of metallic nanoparticles. *International Journal of Molecular Sciences*. 18, 1–21. <https://doi.org/10.3390/ijms18010120>
- Dos Santos, W.G., Pacheco, I., Liu, M.Y., Teixeira, M., Xavier, A.V., LeGall, J., 2000. Purification and characterization of an iron superoxide dismutase and a catalase from the sulfate-reducing bacterium *Desulfovibrio gigas*. *Journal of Bacteriology*. 182, 796–804. <https://doi.org/10.1128/JB.182.3.796-804.2000>
- Duport, C., Jobin, M., Schmitt, P., 2016. Adaptation in *Bacillus cereus*: from stress to disease. *Frontiers in Microbiology*. 7, 1–18. <https://doi.org/10.3389/fmicb.2016.01550>
- Duraivel, S., Shaheda, S.A., Basha, S.R., Pasha, S.E., Jilani, S., 2014. Formulation and evaluation of antiwrinkle activity of cream and nano emulsion of *Moringa oleifera* seed oil. *IOSR Journal of Pharmacy and Biological Sciences*. 9, 58–73. <https://doi.org/10.9790/3008-09415873>
- Fan, Y., Marioli, M., Zhang, K., 2021. Analytical characterization of liposomes and other lipid nanoparticles for drug delivery. *Journal of Pharmaceutical and Biomedical Analysis*. 192, 113642. <https://doi.org/10.1016/j.jpba.2020.113642>
- Filipczak, N., Pan, J., Yalamarty, S.S.K., Torchilin, V.P., 2020. Recent advancements in liposome technology. *Advanced Drug Delivery Reviews*. 156, 4–22. <https://doi.org/10.1016/j.addr.2020.06.022>
- Handayani, I., Saad, H., Ratnakomala, S., Lisdiyanti, P., Kusharyoto, W., Krause, J., Kulik, A., Wohlleben, W., Aziz, S., Gross, H., Gavriilidou, A., Ziemert, N., Mast, Y., 2021. Mining Indonesian microbial biodiversity for novel natural compounds by a combined genome mining and molecular networking approach. *Marine Drugs*. 19, 1–27. <https://doi.org/10.3390/md19060316>
- Honary, S., Zahir, F., 2013. Effect of zeta potential on the properties of nano-drug delivery systems-a review (Part 1). *Tropical Journal of Pharmaceutical Research*. 12, 255–264. <https://doi.org/10.4314/tjpr.v12i2.19>
- Hou, X., Qiu, X., Wang, Y., Song, S., Cong, Y., Hao, J., 2022. Application and efficacy of melatonin elastic liposomes in photoaging mice. *Oxidative Medicine and Cellular Longevity*. 2022, 1-15. <https://doi.org/10.1155/2022/7135125>
- Indrayati A, Asyarie, S., Suciati, T., D.S.R., 2016. Pengaruh superoksida dismutase rekombinan *Staphylococcus equorum* terhadap viabilitas sel dan deposisi kolagen pada sel fibroblas 3T3 yang dipaparkan UVA. *Jurnal Farmasi Indonesia*. 13, 34–40.
- Kang, Y.M., Hong, C.H., Kang, S.H., Seo, D.S., Kim, S.O., Lee, H.Y., Sim, H.J., An, H.J., 2020. Anti-photoaging effect of plant extract fermented with *Lactobacillus buchneri* on CCD-986sk fibroblasts and HaCaT keratinocytes. *Journal of Functional Biomaterials*. 11, 1–12. <https://doi.org/10.3390/jfb11010003>
- Karn, P.R., Cho, W., Park, H.J., Park, J.S., Hwang, S.J., 2013. Characterization and stability studies of a novel liposomal cyclosporin a prepared using the supercritical fluid method: comparison with the modified conventional Bangham method. *International Journal of Nanomedicine*. 8, 365–377. <https://doi.org/http://dx.doi.org/10.2147/IJN.S39025>
- Lee, K.O., Kim, S.N., Kim, Y.C., 2014. Anti-wrinkle effects of water extracts of teas in hairless mouse. *Toxicological Research*. 30, 283–289. <https://doi.org/10.5487/TR.2014.30.4.283>
- Lee, M.J., Agrahari, G., Kim, H.Y., An, E.J., Chun, K.H., Kang, H., Kim, Y.S., Bang, C.W., Tak, L.J., Kim, T.Y., 2021. Extracellular superoxide dismutase prevents skin aging by promoting collagen production through the activation of AMPK and Nrf2/HO-1 cascades. *Journal of Investigative Dermatology*. 141, 2344-2353. e7. <https://doi.org/10.1016/j.jid.2021.02.757>
- Liu, B., Talukder, M.J.H., Terhonen, E., Lampela, M., Vasander, H., Sun, H., Asiegbu, F., 2020. The microbial diversity and structure in peatland forest in Indonesia. *Soil Use and Management*. 36, 123–138. <https://doi.org/10.1111/sum.12543>
- Liu, J., Cui, X., Liu, Z., Guo, Z., Yu, Z., Yao, Q., Sui, Y., Jin, J., Liu, X., Wang, G., 2019. The diversity and geographic distribution of cultivable bacillus-like bacteria across black soils of northeast China. *Frontiers in Microbiology*. 10, 1–11. <https://doi.org/10.3389/fmicb.2019.01424>
- Lujan, H., Griffin, W.C., Taube, J.H., Sayes, C.M., 2019. Synthesis and characterization of nanometer-sized liposomes for encapsulation and microrna transfer to breast cancer cells. *International Journal of Nanomedicine*. 14, 5159–5173. <https://doi.org/10.2147/IJN.S203330>
- Maeda, K., 2018. Analysis of ultraviolet radiation wavelengths causing hardening and reduced elasticity of collagen gels *in vitro*. *Cosmetics*. 5, 1-14. <https://doi.org/10.3390/cosmetics5010014>
- Manosroi, A., Chutoprapat, R., Abe, M., Manosroi, W., Manosroi, J., 2012. Anti-aging efficacy of topical formulations containing niosomes entrapped with rice bran bioactive compounds. *Pharmaceutical Biology*. 50, 208–224. <https://doi.org/10.3109/13880209.2011.596206>
- Shazeeb, M.S., Feula, G., Jr, A.B., 2014. Liposome-encapsulated superoxide dismutase mimetic: theranostic potential of an MR detectable and neuroprotective agent. *National Institutes of Health*. 9, 221–228. <https://doi.org/10.1002/cmimi.1559>

- Naibaho, J., Safithri, M., Wijaya, C.H., 2019. Anti-hyperglycemic activity of encapsulated Java tea-based drink on malondialdehyde formation. *Journal of Applied Pharmaceutical Science*. 9, 88–95. <https://doi.org/10.7324/JAPS.2019.90411>
- Najmuldeen, H., Alghamdi, R., Alghofaili, F., Yesilkaya, H., 2019. Functional assessment of microbial superoxide dismutase isozymes suggests a differential role for each isozyme. *Free Radical Biology and Medicine*. 134, 215–228. <https://doi.org/10.1016/j.freeradbiomed.2019.01.018>
- Nurfitriyawati, N., Indrayati, A., Rukmana, R.M., Haryanti, S., 2023a. Antiphotoreaging effects of liposomal encapsulated superoxide dismutase extract of *Bacillus altitudinis* on ultraviolet-A-irradiated New Zealand rabbits' back skin. *Journal of Applied Pharmaceutical Science*. 13, 144–150. <https://doi.org/10.7324/japs.2023.113079>
- Nurfitriyawati, Indrayati, A., Maarif, R.R., 2023b. Karakteristik enkapsulasi liposom ekstrak superoksida dismutase (SOD) *Bacillus altitudinis*. *Jurnal Ilmiah Ibnu Sina*. 8, 21–30. <https://doi.org/https://doi.org/10.36387/jiis.v8i1.1078>
- Petkar, M.B., Pillai, M.M., Kulkarni, A.A., Bondre, S.H., Rao, K.R.S.S., 2013. Purification and characterization of superoxide dismutase isolated from sewage isolated *E. coli*. *Journal of Microbial and Biochemical Technology*. 5, 102–106. <https://doi.org/10.4172/1948-5948.1000109>
- Porfire, A.S., Pärvu, A.E., Daicovicu, D., Leucuța, S.E., 2009. Evaluation of antiinflammatory activity of liposome encapsulated superoxide dismutase in rats peritonitis. *Farmacia*. 57, 412–423.
- Priadi, G., Setiyoningrum, F., Afiati, F., 2018. Enzim β -Galaktosidase dari *Leuconostoc mesenteroides* indigenus: ekstraksi, purifikasi parsial dan karakterisasi. *Prosiding Seminar Nasional Masyarakat Biodiversitas Indonesia*. 4, 184–189. <https://doi.org/10.13057/psnmbi/m040215>
- Richmond, J.M., Harris, J.E., 2014. Immunology and skin in health and disease. *Cold Spring Harbor Perspectives in Medicine*. 4, 1–20. <https://doi.org/10.1101/cshperspect.a015339>
- Stelder, S.K., Benito De Moya, C., Hoefsloot, H.C.J., De Koning, L.J., Brul, S., De Koster, C.G., 2018. Stoichiometry, absolute abundance, and localization of proteins in the *Bacillus cereus* spore coat insoluble fraction determined using a QconCAT approach. *Journal of Proteome Research*. 17, 903–917. <https://doi.org/10.1021/acs.jproteome.7b00732>
- Suksaeree, J., Kantapak, K., Sansiri, P., Chatpitukpong, N., Kajornwongwattana, W., 2018. Skin irritation test of Thai herbal face wash gel formulations using the New Zealand white rabbits. *Thai Journal of Pharmaceutical Sciences*. 42, 93–97.
- Sun, M., Ye, S., Xu, Z., Wan, L., Zhao, Y., 2021. Endophytic *Bacillus altitudinis* Q7 from Ginkgo biloba inhibits the growth of *Alternaria alternata* in vitro and its inhibition mode of action. *Biotechnology and Biotechnological Equipment*. 35, 880–894. <https://doi.org/10.1080/13102818.2021.1936639>
- Novarini, T., Indrayati, A., Purwaningsih, D., 2020. Activity assay of superoxide dismutase (SOD) enzyme in the extract of temu hitam (*Curcuma aeruginosa* Roxb.) with water soluble tetrazolium salt-1 (WST-1) method. *Jurnal Sains Dan Kesehatan*. 3, 242–247.
- Tran, H.M., Yang, C.Y., Wu, T.H., Yen, F.L., 2022. Liposomes encapsulating morin: investigation of physicochemical properties, dermal absorption improvement and anti-Aging activity in PM-induced keratinocytes. *Antioxidants*. 11, 1–21. <https://doi.org/10.3390/antiox11061183>
- Treiber, N., Maity, P., Singh, K., Ferchuu, F., Wlaschek, M., Scharffetter-Kochanek, K., 2012. The role of manganese superoxide dismutase in skin aging. *Dermato-Endocrinology*. 4, 232–235. <https://doi.org/10.4161/derm.21819>
- Ukeda, H., Kawana, D., Maeda, S., Sawamura, M., 1999. Spectrophotometric assay for superoxide dismutase based on the reduction of highly water-soluble tetrazolium salts by xanthine-xanthine oxidase. *Bioscience, Biotechnology and Biochemistry*. 63, 485–488. <https://doi.org/10.1271/bbb.63.485>
- Vorauer-Uhl, K., Fürnschliel, E., Wagner, A., Ferko, B., Katinger, H., 2001. Topically applied liposome encapsulated superoxide dismutase reduces postburn wound size and edema formation. *European Journal of Pharmaceutical Sciences*. 14, 63–67. [https://doi.org/10.1016/S0928-0987\(01\)00149-X](https://doi.org/10.1016/S0928-0987(01)00149-X)
- Wang, Y., Mo, X., Zhang, L., Wang, Q., 2011. Four superoxide dismutase (isozymes) genes of *Bacillus cereus*. *Annals of Microbiology*. 61, 355–360. <https://doi.org/10.1007/s13213-010-0149-6>
- Younus, H., 2018. Therapeutic potentials of superoxide dismutase. *International Journal of Health Sciences*. 12, 88–93.
- Yun, X., Maximov, V.D., Yu, J., Zhu, H., Vertegel, A.A., Kindy, M.S., 2013. Nanoparticles for targeted delivery of antioxidant enzymes to the brain after cerebral ischemia and reperfusion injury. *Journal of Cerebral Blood Flow and Metabolism*. 33, 583–592. <https://doi.org/10.1038/jcbfm.2012.209>
- Zhang, J., Wang, H., Huang, Q., Zhang, Y., Zhao, L., Liu, F., Wang, G., 2020. Four superoxide dismutases of *Bacillus cereus* 0–9 are non-redundant and perform different functions in diverse living conditions. *World Journal of Microbiology and Biotechnology*. 36, 1–12. <https://doi.org/10.1007/s11274-019-2786-7>
- Zhang, S., Duan, E., 2018. Fighting against skin aging: the way from bench to bedside. *Cell Transplantation*. 27, 729–738. <https://doi.org/10.1177/0963689717725755>